

Interaction between telencephalic signals and respiratory dynamics in songbirds

Jorge M. Méndez,¹ Gabriel B. Mindlin,² and Franz Goller¹

¹Department of Biology, University of Utah, Salt Lake City, Utah; and ²Physics Department, Universidad de Buenos Aires, Buenos Aires, Argentina

Submitted 11 July 2011; accepted in final form 1 March 2012

AQ: 1

AQ: 2

Méndez JM, Mindlin GB, Goller F. Interaction between telencephalic signals and respiratory dynamics in songbirds. *J Neurophysiol* 107: 000–000, 2012. First published March 7, 2012; doi:10.1152/jn.00646.2011.—The mechanisms by which telencephalic areas affect motor activities are largely unknown. They could either take over motor control from downstream motor circuits or interact with the intrinsic dynamics of these circuits. Both models have been proposed for telencephalic control of respiration during learned vocal behavior in birds. The interactive model postulates that simple signals from the telencephalic song control areas are sufficient to drive the nonlinear respiratory network into producing complex temporal sequences. We tested this basic assumption by electrically stimulating telencephalic song control areas and analyzing the resulting respiratory patterns in zebra finches and in canaries. We found strong evidence for interaction between the rhythm of stimulation and the intrinsic respiratory rhythm, including naturally emerging subharmonic behavior and integration of lateralized telencephalic input. The evidence for clear interaction in our experimental paradigm suggests that telencephalic vocal control also uses a similar mechanism. Furthermore, species differences in the response of the respiratory system to stimulation show parallels to differences in the respiratory patterns of song, suggesting that the interactive production of respiratory rhythms is manifested in species-specific specialization of the involved circuitry.

birdsong; respiration; vocal control; nonlinear dynamics; entrainment

AQ: 3

WHEREAS ANATOMICAL CONNECTIONS from cortical areas of the brain to diverse peripheral effectors have been characterized in detail, the mechanisms by which they exert control over motor circuits are poorly understood (see, e.g., Capaday 2004; Lemon 2008; Riddle and Baker 2010; Soto and Cros 2011). Views of how these areas interact with downstream circuits range from a direct takeover of motor control (Ahrens and Kleinfeld 2004; Berg and Kleinfeld 2003; Kakei et al. 1999) to a more modulatory, interactive role (Cramer and Keller 2006; Friedman et al. 2006; Lang et al. 2006; Marshall and Lang 2004). Voluntary control of respiration is an interesting motor system for exploration of this issue, as it affects an involuntary function and therefore must integrate the physiological constraints of gas exchange (Miller et al. 1997). In addition, respiratory rhythms are coordinated with a number of other motor activities, such as locomotion, swallowing, etc., and their respective rhythms (Bramble and Carrier 1983; Funk et al. 1992; Miller et al. 1997; Potts et al. 2005), thus indicating that different modulatory influences on the pattern generating circuits of respiration exist (Rekling and Feldman 1998).

Telencephalic control of learned vocal behavior constitutes one such pathway that requires alteration of a normal respira-

tory rhythm (Butler 2007; Corfield et al. 1998; Goller and Cooper 2004; Haouzi and Bell 2009). In many songbirds, respiratory rhythms lay the foundation for the elaborate temporal patterns of song (Suthers et al. 1999). Respiratory patterns of song vary substantially between different species. Some species sing songs that are generated by a series of different, individual expiratory pressure pulses that alternate with mostly silent, short inspirations (minibreaths). An example for this song organization is found in the zebra finch (*Taeniopygia guttata*). Other species sing songs with repeated acoustic elements (trills), which are generated with stereotyped sequences of modulated respiratory pressure. Canary (*Serinus canaria*) song, for example, contains trills with different sound pulse frequencies generated by sequences of different respiratory rhythms (see, e.g., Hartley and Suthers 1989; Suthers et al. 2004). How do telencephalic song control centers interact with the respiratory network to generate these respiratory patterns of song?

In songbirds, song production is controlled by a motor circuit, including telencephalic nuclei HVC (used as a proper name) and robust nucleus of the arcopallium (RA). RA connects directly to the motor nucleus (hypoglossal nucleus) for control of muscles of the vocal organ, the syrinx, and to the premotor areas with putative central pattern generators (CPGs) for respiration (Wild 1997; Zeigler and Marler 2008). Whereas a more complete anatomical description of all components of the circuitry is emerging (for a detailed figure see Fig. 8 in Wild et al. 2009), our understanding of the functional roles of the extended network is still primitive.

It has been argued for zebra finch song that all major temporal features of song are included in the instructions from this telencephalic motor circuit (Hahnloser et al. 2002; Long and Fee 2008). Under this model, a small group of RA-projecting neurons in HVC activate a subset of neurons in RA, which then through their convergence onto the motor systems produce the song instructions. A one-to-one correspondence between the firing of a specific sequence of RA-projecting HVC neurons and a specific motor instruction is established, with no time features arising from processing of these instructions in the downstream network. This model was recently modified based on respiratory data to allow a role of the respiratory network for modifying the dynamics of air sac pressure during silent intersyllable inspirations. The timing of expirations, during which sounds are produced, and the on- and offset of inspirations are still thought to be controlled directly by HVC (Andalman et al. 2011).

Alternatively, instructions from this forebrain motor circuit could interact with the intrinsic dynamics of the respiratory

AQ: 11

Address for reprint requests and other correspondence: F. Goller, Dept. of Biology, Univ. of Utah, Salt Lake City, UT, 84112 (e-mail: goller@biology.utah.edu).

AQ: 11

network to generate the elaborate temporal patterns of respiration during song in canaries (Trevisan et al. 2006a). This latter hypothesis predicts that respiratory rhythms do not merely reflect the temporal sequence of telencephalic input into the medullary control network but contain the signature of interactive processing.

The complexity of motor control of song production makes it difficult to experimentally test the interactive hypothesis during spontaneously generated behavior. However, the basic assumptions of the interactive processing hypothesis can be tested directly. The effects of stimulating the telencephalic song control areas on respiration can be used to assess the validity of the interaction hypothesis. If the results of such an experiment show uncoordinated dynamics between the telencephalic input and respiration (absence of mixing between the imposed telencephalic frequency and the respiratory rhythm), the interactive hypothesis is refuted. Overall, this scenario would provide support for the notion that overriding control of brain stem circuitry by the forebrain is possible. If, on the other hand, the telencephalic instructions (an artificial rhythm created by electrical stimulation) interact with the respiratory dynamics, the resulting respiratory patterns should display clear fingerprints of this integration, such as subharmonic behavior. The behavior emerging from this interaction could be linear, in which case the respiratory rhythm should always follow the rhythm of the telencephalic input (forcing) in a 1:1 correspondence. In a nonlinear system, a 1:1 correspondence between the forcing and the final response of the forced system can also be found, but only for a bounded range of forcing parameters (i.e., when the forcing frequency is close to that of the natural rhythm of the driven system). If the forcing frequency is very different from the natural frequency, more complex solutions are expected. Among these stand the so-called subharmonic solutions, which present periodic responses with periods that are multiples of the forcing period (i.e., the forcing frequency is close to an integer multiple of the natural frequency of the driven system, e.g., 1:2, 1:3) (Pipes and Harvill 1946). A more complex response is the ultrasubharmonic responses of order n , m , which occur when the forcing frequency and the natural frequency of the driven system are related in other integer ratios (e.g., 2:3) (Wiggins 2003). If the telencephalic instructions interact with the respiratory rhythm generator in this fashion, we expect telencephalic stimulation to elicit these complex patterns. This means that pressure patterns should emerge such that their periods are multiples of the period of the stimulation across a broad range of the forcing parameters. Here we report the results of this first critical experiment in testing the interactive model. The data show clear evidence for integration of telencephalic stimulation and respiratory dynamics.

METHODS

Animals. We used 15 adult male zebra finches and 5 adult male canaries in this study. Zebra finches were raised in an aviary, while canaries were purchased from a local dealer. All animals were kept alive after this experiment for chronic recording of air sac pressure and spontaneously generated song.

Surgical procedure and recording. All experimental procedures were approved by the Institutional Animal Care and Use Committee (IACUC) of the University of Utah.

Air sac pressure recording. The surgical procedures and recording methods were previously described in detail (Goller and Suthers 1996a, 1996b). In summary, an elastic belt with a Velcro tab was fitted around the bird's thorax to which a wire was attached for tethering the bird to a counterbalanced tether arm. After the birds resumed singing, the surgical procedure was carried out. The bird was deprived of food and water for 1 h before the surgery. Under isoflurane anesthesia, a small hole was made in the abdominal wall and a flexible cannula (Silastic tubing, Dow Corning, Midland, MI) was inserted into an anterior thoracic air sac. The cannula was sutured to the ribs, and the free end of the cannula was connected to a pressure transducer (Fujikura FPM-02PG, Tokyo, Japan) mounted on the backpack.

Chronic electrode implants. The experimental methods used for the chronic electrode implants were based on the procedure used by Ashmore et al. (2005). Zebra finches and canaries were anesthetized with a mixture of ketamine and xylazine (ketamine HCl-xylazine HCl solution, K-113, Sigma, St. Louis, MO). After reaching a sufficient level of deep anesthesia, the bird was placed in the stereotaxic apparatus (Myneurolab, Richmond, IL). HVC and RA were identified by their stereotaxic coordinates and by the characteristic firing patterns of the neurons in these regions. For electrophysiological recordings 1-M Ω tungsten electrodes were used (Microprobe) and inserted into the approximate area of HVC and RA with stereotaxic coordinates. The region was then identified by the characteristic firing patterns of neurons. At a variable number of positions within the nucleus we tested acutely for entrainment, exploring the dorso-ventral and lateral axes of the nucleus. Once the acute test was finished, a set of bipolar electrodes for stimulation were implanted in the core of the previously explored and identified area approximately in a central position in respect to the dorso-ventral and lateral edges of the nucleus. To further verify the placement of the stimulation electrodes, we applied an electrical stimulation of not more than 20 μ A. If a small fluctuation in air sac pressure resulted from this stimulus, we concluded that the electrode was placed in a song control nucleus. The electrodes were made from Formvar-insulated nichrome wire of 25 μ m (A-M Systems, Carlsborg, WA) and had a typical impedance of \sim 500 k Ω at 1 kHz (LCR-817, GW Instek, Chino, CA). The electrodes were connected to a microconnector (Omnetics, Minneapolis, MN), which was cemented to the skull with dental cement (Lang Dental, Wheeling, IL).

Electrical microstimulation. Three stimulation protocols were used. Single-train stimulation consisted of 10 monophasic pulses of 200 μ s with a current from 5 to 500 μ A and a frequency of 200 Hz. Periodic stimulation was performed by continuously repeating the train of 10 pulses after a time T_f (frequency of the forcing is the inverse of this time). The duration of the periodical stimulation was variable but always less than a minute. The third stimulation regime consisted of a long-duration continuous stimulation. The duration of the stimulation was adjusted according to the number of pulses applied per continuous stimulation bout. The same pulse characteristics were used for all three protocols.

Chronic recording of pressure and telencephalic stimulation. The bird was placed in a cage with a miniature slip-rig commutator (Dragonfly, Ridgeley, WV), allowing free movement by the bird. The pressure transducer was connected to an amplifier circuit (Hector Engineering, Ellettsville, IN). The stimulation was performed with one or two isolated current stimulators (DS3, Digitimer, Welwyn Garden City, UK) that were triggered by either a computer with a custom LabVIEW (National Instruments, Austin, TX) program or a function generator (33220A, Agilent, Santa Clara, CA). The trigger signal and the air sac pressure recordings were simultaneously recorded with a computer (Avisoft Recorder software).

Analysis methods. All analysis methods were programmed in MATLAB (version 7.7.0, MathWorks, Natick, MA).

Relative phase to account for phase synchronization. The phase of the pressure pattern $[\theta_p(t)]$ was calculated by taking the Hilbert transformation of its time series (for a detailed explanation of how to

calculate the transformation see Osipov et al. 2007). Basically, the Hilbert transformation is a method for extracting the phase and amplitude from a time series of a variable with oscillatory characteristics. Entrainment implies a relationship between the phase of the pressure pattern and the corresponding phase of the forcing signal. Then for each integer value of n and m the phase difference was calculated as

$$\Phi_{nm}(t) = n\phi_p(t) - \frac{2\pi m}{T_f}t$$

where T_f is the forcing period (Osipov et al. 2007). To clarify this equation, suppose that the pressure pattern is periodic in such a way that it repeats itself after two periods of the forcing signal, and in this time it only presents one inspiration; this pattern is formally represented as 1:2 entrainment. In the same amount of time in which the pressure pattern phase undergoes a complete turn (2π), the forcing phase undergoes two turns (4π). In a condition of perfect 1:2 entrainment and taking $m = 1$ and $n = 2$, the phase difference would be constant. A graphic way to visualize entrainments is to plot the phase difference in time for different integers, where entrainments correspond to horizontal lines. In general, entrainments are not perfect, in which case horizontal lines would be interrupted from time to time until a new or the same entrainment is reestablished.

Sign of the air sac pressure pattern fluctuation. To calculate the sign of the pressure fluctuation for each stimulation, three points of the time series were taken. If t_s represents the time of the electrical stimulation, one vector is made by taking $A_s = (t_s + 20 \text{ ms}, p(t_s + 20 \text{ ms}))$. Then taking t between $t_s + 20 \text{ ms}$ and $t_s + 70 \text{ ms}$, if t_{\max} is the value of t in which $p(t) - p(t_s + 20 \text{ ms})$ is maximal the vector $A_{\max} = (t_{\max}, p(t_{\max}))$ is built. Finally, the vector $B = (t_s + 70 \text{ ms}, p(t_s + 70 \text{ ms}))$ is considered. To compute the sign, the following cross product is calculated:

$$\frac{B - A_s}{\|B - A_s\|} \times \frac{A_{\max} - A_s}{\|A_{\max} - A_s\|}$$

The sign of this product gives the sign of the pressure fluctuation, and we called it relative amplitude.

Return map. A simple way to extract periodicities from a time series is to plot a return map. To build a return map from the pressure pattern time series, we selected a value and the corresponding direction of the flow (positive derivative) at this value. Each time the pressure pattern crossed this value with the correct flow direction, the time of that crossing is computed (t_n). Then the following time differences are calculated:

$$T_n = T_{n+1} - t_n$$

The return map is the plot of T_{n+1} vs. T_n . If the pressure pattern is a periodic pattern, a cloud of points will appear tightly clustered around the period of that pattern.

Relative pressure amplitude. To compare the pressure amplitude caused by stimulation to the pressure values during normal breathing before stimulation, the following quantifier was calculated. To calculate a baseline pressure amplitude for a stimulation period of T_f , the pressure pattern corresponding to normal breathing before stimulation was used to calculate

$$B = \frac{1}{n} \int_0^{nT_f} |p(t)| dt$$

where n is the number of periods used for the calculation, and p is the pressure in which zero represents the atmospheric level.

If the whole stimulation consists of N single stimulations starting at time T_i , for each stimulation period that is the time between two single stimulations the following quantifier is calculated (for example, if it is calculated for period k , the time between stimulation $k - 1$ and k is considered)

$$PA(k) = \frac{1}{B} \int_{T_i+(k-1)T_f}^{T_i+kT_f} |p(t)| dt$$

This quantifier provides a way to compare the fluctuation produced by the stimulation in each period of the stimulation.

RESULTS

In awake male zebra finches (*T. guttata*) and canaries (*S. canaria*) with previously implanted stimulation electrodes in HVC or in RA, we applied a stimulation protocol that incorporated an individual pulse train, pulse trains with different rhythms, and a continuous, long-duration train of pulses. To assess respiratory dynamics we recorded subsyringeal pressure by cannulating a thoracic air sac.

The response of the respiratory system is phase dependent. Electrical stimulation at relatively low currents in HVC and in RA resulted in a distinct change in respiratory pressure. With the exception of one bird, individual pulses of stimulation caused an increase in air sac pressure starting ~ 20 ms after the onset of stimulation (Fig. 1A), indicating activation of the expiratory nucleus of the respiratory circuitry (nu-

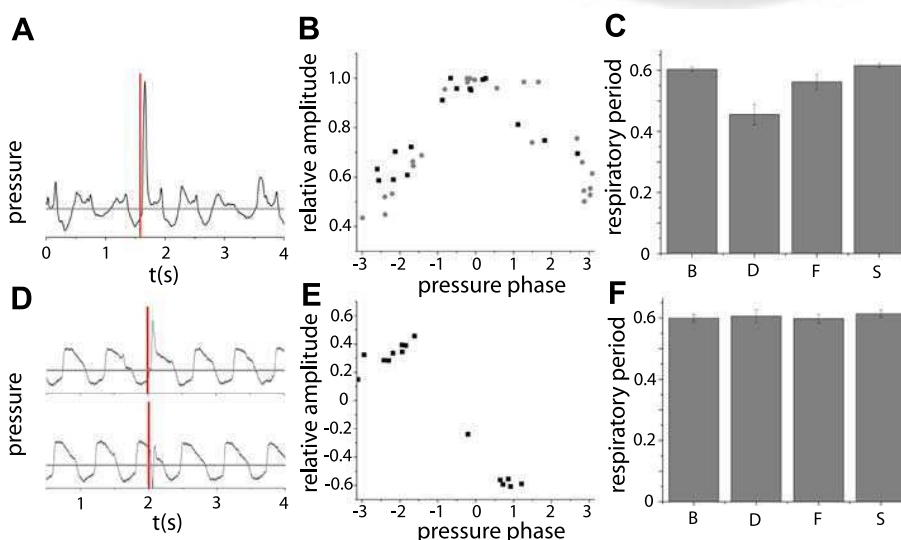


Fig. 1. Response to telencephalic stimulation is phase dependent. **A:** representative example from a zebra finch (ZF1). Air sac pressure (black; gray line indicates atmospheric level) increases sharply after stimulation (red). **B:** amplitude changes caused by stimulation are dependent on when the stimulation occurred during the respiratory cycle. This effect was quantified by the calculation of the relative amplitude as a function of the pressure phase. Results of the stimulations with $50 \mu\text{A}$ at 2 different positions within left RA ($100 \mu\text{m}$ apart) are displayed in black and in gray. **C:** duration of respiration is affected by stimulation. **B,** respiratory period before stimulation; **D,** respiratory period in the cycle when stimulations happened; **F,** respiratory period during 1st cycle after stimulation; **S,** respiratory period during 2nd cycle after stimulation. **D–F:** air sac pressure in only 1 bird (canary, CAN2) responded to stimulation with a negative fluctuation during some phases of the respiratory cycle. In **D** 2 examples showing a positive and a negative fluctuation are displayed ($20 \mu\text{A}$, left RA). The pressure phase was calculated by means of a Hilbert transformation of the original pressure pattern time series.

cleus retroambiguus, RA_m). In general, a 20- μ A stimulation was enough to trigger a positive pressure fluctuation. Even though in most cases we did not collect enough data to build a map like that displayed in Fig. 1B, this observation was consistent across anesthetized birds. The exceptional bird (CAN2, awake with a unilateral chronic implant in RA) showed a decrease in air sac pressure during a part of the expiratory phase, which might indicate a stimulation of the inspiratory network (Fig. 1D). The amplitude of the induced pressure change was dependent on the phase relationship between stimulus and expiratory cycle (Fig. 1, B and E). In some cases, the telencephalic stimulation was able to change the respiratory period, which represents evidence for an integration of this signal by the brain stem circuitry (Fig. 1C). In the case shown in Fig. 1C, the differences in the respiratory period before and during the respiratory cycle of the stimulation were significant (Student's *t*-test, $P < 0.05$). Therefore, the phase dependence of the response and the effect on the respiratory cycle period are evidence that the stimulation is not processed as an additive perturbation.

Stimulation at two different locations within RA (at least 200 μ m apart in the lateral direction) elicited a similar response in respiration (Fig. 1B). The electrodes were positioned to supposedly activate different sets of RA neurons (Histed et al. 2009). We did not discriminate between dorsal and ventral RA, which have been affiliated with respiratory and syringeal premotor control, respectively (Vicario 1991). Notably, even when very low stimulation currents (10 μ A) were applied through one electrode set, there was a change in neural activity in other set in the same nucleus, indicating that uniform activation may have been caused by the interconnections within this nucleus. The similar effect of stimulation in both areas suggests a population level control of motor gestures.

Exploration of responses at different electrode positions was made in each bird during anesthesia (acute test), but as these were mostly used for identification of the boundaries of the respective nucleus for electrode implantation for the chronic test, we did not systematically explore the whole nucleus (as shown in Fig. 1B) in all birds. Nevertheless, in all cases a positive response was observed.

Periodic stimulation of telencephalic nuclei creates subharmonic entrainments. The nonlinear characteristics of the respiratory network were illustrated by periodic stimulation of the telencephalic areas (see METHODS). Whereas a 1:1 entrainment is also consistent with a direct control mechanism, the occurrence of respiratory frequencies that are subharmonics of the

stimulation frequency is evidence of 1) interactive and 2) nonlinear behavior. Subharmonic entrainments were obtained in all birds, and the exact entrainment regime depended on the difference in frequency between prestimulation respiration and electrical stimulation. For example, when the stimulation frequency was close to the respiratory frequency, respiration got locked 1:1 to the stimulation. As the stimulation frequency was increased, other higher-order entrainments were obtained, following the well-described Arnold tongues (Feingold et al. 1988; Glass 2001; Gonzalez and Piro 1983; Wiggins 2003) (Fig. 2). An Arnold tongue is a region of the parameter space, in this case the current and period of the stimulation, in which a stable entrainment is established. When the stimulation frequency was close to twice the respiratory frequency, respiration was entrained to a 1-to-2 ratio, i.e., a so-called period 2 solution in which the respiration repeats itself after twice the forcing period (Fig. 2). More complex solutions also arose, such as the 2:3 relationship (explained above as ultrasubharmonic solutions), which was obtained with stimulation frequencies in between those that resulted in the 1:1 and the 1:2 solutions (Fig. 2D). The general occurrence of entrainments in our experiments for zebra finches and canaries is summarized in Table 1. Figure 2A displays an example for a zebra finch with a chronic unilateral implant in RA, in which different entrainments were obtained when the frequency of stimulation was changed. When the stimulation period was 0.3 s, a 1:1 entrainment was obtained, because it was close to the period of quiet respiration (0.45 s). With a stimulation period (0.2 s) close to half of the respiratory period, a 1:2 entrainment was observed, and a further reduction of the period to 0.12 s gave rise to a 1:3 entrainment. Stimulation affected respiration frequency (Fig. 2B), indicating that the entrainments are not passively established. The order of appearance of the entrainments is the expected order in a nonlinear oscillator under an external forcing. As the stimulation frequency was increased, higher subharmonics were observed (Fig. 2C), and between the 1:1 and the 1:2 the 2:3 subharmonic occurred (Fig. 2E).

In addition to the observed entrainment regimes following stimulation of telencephalic song control centers, the effects of stimulation on air sac pressure amplitude were also consistent with the interactive model. In some cases, the amplitude of entrained air sac pressure pulses changed only slightly compared with that during normal, quiet breathing (Fig. 2A). In other cases, however, the amplitude of both expiratory and inspiratory pulses was drastically increased and reached values that are typical of song (Fig. 2F). The songlike pressure

Fig. 2. Entrainments of the respiratory rhythm to the stimulation. A, D, and F: examples of entrainments of the respiratory patterns for a zebra finch (ZF4) with small change of the pressure pattern amplitude (A), for a canary (CAN2) (D), and for a canary (CAN3) with large-amplitude pressure patterns (F). To illustrate the difference in amplitude, the atmospheric level is displayed as a dashed gray line and the mean level of expiration and inspiration during quiet breathing in solid gray lines (right). Different stimulation frequencies gave rise to different entrainment ratios: 1:1, 1:2, 1:3. In A, the period of quiet breathing was ~ 0.45 s. The stimulation (20 μ A) with a period of 0.3 s entrained respiration to a 1:1 rhythm. When the stimulation period was reduced to 0.2 s, the entrainment ratio changed to 1:2, and with 0.12 s it was 1:3. The entrainments were visualized by calculating relative phases (see METHODS). The segments of the time series displayed on right are indicated in red by the line representing the relative phase. Red vertical lines on right indicate the stimulation. Blue lines on left correspond to the relative phase calculated with surrogate data taken from a pressure time series before the stimulation for A and the segments of the time series immediately before and after the stimulation as surrogate for the entrainments for D and F. B: power spectrum of the pressure patterns for each of the displayed entrained conditions (1:1, 1:2, and 1:3). Quiet breathing frequency increased slightly as a result of the stimulation period. C: relationships between the respiratory frequency (f_{resp} , quiet breathing immediately before the stimulation), the stimulation frequency (f_s), and the peak frequency of the power spectrum (f_{max}) for A. D: different stimulation frequencies gave rise to different entrainment ratios: 1:1, 2:3, 1:2. The period of the quiet breathing rhythm differed slightly in each panel: 0.52 s (top), 0.4 s (middle), or 0.45 s (bottom). Stimulation periods were 0.4, 0.25, and 0.18 s, respectively, and stimulation current was 100 μ A. E: frequency relationships for D. First entrainment sequence shown in F contains a change of entrainment that could be the result of a stimulation-mediated change in the breathing rhythm. This transition is indicated by a black arrow in the part of the figure that relates the different frequencies in G.

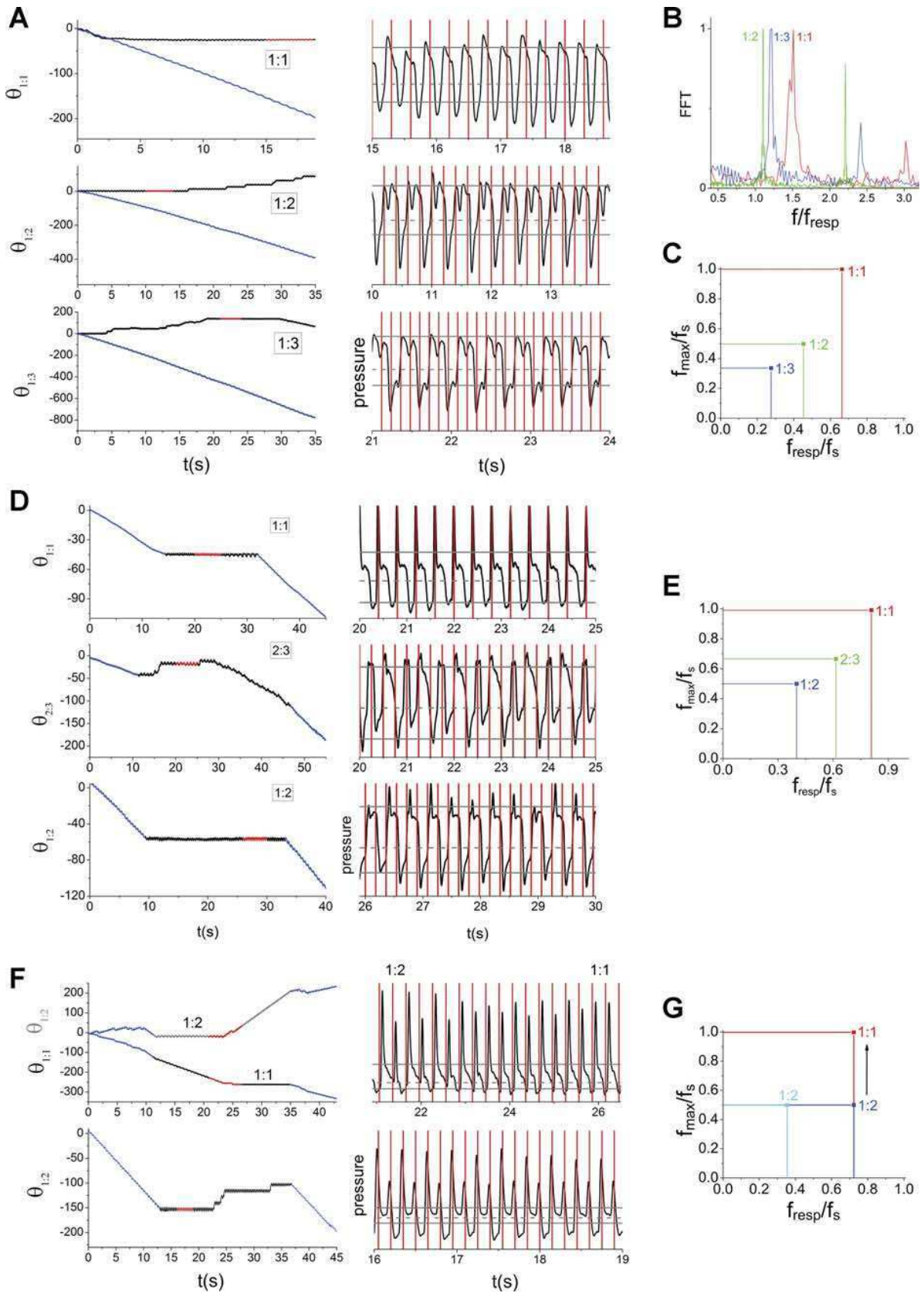


Table 1. Detailed description of entrainment occurrence

Bird	Stimulation Site	State	Current Range, μA	Entrainment Success	Entrainment Ratios
ZF1	RA: right (2)	Anesthetized	20–100	8/14	1:1, 1:2
ZF7	RA bilateral	Anesthetized	10–100	6/7	1:1, 1:2, 2:2, pulsatile
ZF8	RA: right	Anesthetized	100	0/8	–
ZF10	HVC: left (2)	Anesthetized	100–500	0/6	–
ZF11	HVC: left	Anesthetized	50–500	0/9	–
ZF12	HVC: left	Anesthetized	10–200	0/7	–
ZF4	RA: left	Awake	200	5/6	1:1, 1:2, 1:3, 1:4
ZF5	RA: right	Awake	200	3/3	1:1, 1:2, pulsatile
ZF6	RA: right	Awake	100	5/5	1:1, 1:2, 1:3
ZF8	RA: right	Awake	30–100	31/37	1:1, 1:2, 1:3, 1:4, 1:5, 2:3, pulsatile
ZF9	HVC: left	Awake	100–500	5/10	1:1, 1:2 (T)
ZF13	HVC: right	Awake	50–300	30/38	1:1, 1:2, 1:3, 1:4, 1:5, pulsatile (T)
ZF14	HVC: bilateral	Awake	200	14/14	1:1, 1:2, 1:3, 2:3, 1:4, 1:5, 1:6 (T)
CAN1	RA: right	Anesthetized	100	9/14	1:1, 1:2, 1:3, 2:2
	HVC: right	Anesthetized	300	2/6	1:2
CAN2	RA: right	Awake	100–200	10/12	1:1, 1:2, 2:3, 1:3, pulsatile
CAN3	RA: left	Awake	50–200	9/11	1:1, 1:2, 1:3, 1:4
CAN4	HVC bilateral	Awake	20–100	40/40	1:1, 1:2, 1:3, 1:4, pulsatile
CAN5	HVC: left	Awake	20–100	9/11	1:1, 1:2, 1:3, 1:4, pulsatile

ZF, zebra finch; CAN, canary; T, transient entrainment like those shown in Fig. 3.

amplitude combined with subharmonic temporal patterns provides strong support that telencephalic input interacts with the nonlinear respiratory network. On some occasions, stimulation in zebra finches resulted in transient entrainments (Fig. 3A). Even though the global pressure pattern looks variable, at a shorter timescale it has periods of time in which the pattern is locked to periodic trajectories. For example, Fig. 3A, *left*, shows an entrainment of period 6 (i.e., air sac pressure repeats each 6 periods of the stimulation) followed by a period 3. The stimulation caused a clear change in the respiratory period from 0.53 s before the stimulation to 0.3 s after it (Fig. 3A). The appearance of this transient behavior was observed only when pressure amplitude as a result of stimulation was elevated over levels of quiet respiration (Fig. 3B). In these cases, the stimulation might have triggered a transient behavior of the network originating in the intrinsic network properties. Alternatively, an extrinsic inhibitory input might have reduced the effectiveness of telencephalic control on the network. High-amplitude transient entrainments were only observed in awake animals (Fig. 3 and Table 1).

The occurrence of entrainment was highly state dependent. Although we did not quantify the depth of anesthesia, in anesthetized birds the mean respiratory rhythm was significantly lower (1.66 ± 0.12 Hz) than in awake birds (2.85 ± 0.36 Hz; Student's *t*-test, $P < 0.05$). Birds under the effect of anesthesia were more likely to display uncorrelated responses between the telencephalic signal and respiration or only very brief locked periods (Fig. 4A). Figure 4A illustrates that the respiratory rhythm was clearly affected at the beginning of the stimulation but resumed the original rhythm after a transient period corresponding to several respiratory cycles. This observed pattern resembles a superposition of the normal breathing pattern and the fluctuations caused by the stimulation (Fig. 4A). Plotting the respiratory period of a cycle against the period of its following cycle (return map) provides a way to visualize the stimulation effect. The rhythm was not entrained to any simple n -to- m ratio and returned to the normal breathing rhythm after a transitory period (Fig. 4B). The lack of locking behavior under anesthesia was even present for high stimula-

tion currents (500 μA) (Fig. 4C). Direct comparison of the responses to RA stimulation within one individual illustrates clear entrainment during stimulation with 50 μA in the awake animal but no clear locking at twice the level of stimulation current under anesthesia (Fig. 4D). Under anesthesia, the bird displayed a variable breathing pattern and no stable locking (Fig. 4E), whereas the same bird, when awake, showed a less variable breathing pattern and a 1:2 entrainment (Fig. 4F).

Entrainments are the typical response of the respiratory system. During song, canaries repeat individual respiratory pulses to generate repetitions of individual syllable types and then rapidly switch to another pulse type to produce a different syllable (Hartley and Suthers 1989). A similar pattern resulted from electrical stimulation of telencephalic areas (Fig. 5, A and B). Almost all applied stimulation frequencies gave rise to subharmonic behavior (with different entrainment ratios or rotation numbers; Table 1), indicating only small regions of the parameter space—defined by the amplitude and the frequency of the stimulation (corresponding to the current and the frequency of the electrical stimulation)—with unstable behavior between subharmonics (Fig. 5A). We did not tune the stimulation frequency to obtain the displayed entrainments. Pressure patterns with entrainments of 1:1 (period 1) as well as 1:3 (period 3) and 1:2 (period 2) emerged. Another period 1 solution appeared at higher stimulation frequencies and was accompanied by sustained expiratory pressure that was modulated at the frequency. This solution is reminiscent of period 1 solutions with pulsatile pressure patterns during song (i.e., sustained expirations with rhythmic modulation of pressure amplitude; Allende et al. 2010). A change in frequency of the periodic stimulation created fast transitions between different rhythms of respiration (Fig. 5B). A transition from a stimulation period of 0.6 s (1:1 entrainment, Fig. 5A) to 0.2 s (1:2 entrainment, Fig. 3A) contained a fast songlike transition between both patterns. Such rapid transitions also occur during song in canaries (Hartley and Suthers 1989). This implies that the neural architecture is biased toward the generation of subharmonic behavior so that they are robustly obtained. Furthermore, the fact that the transitions between different entrain-

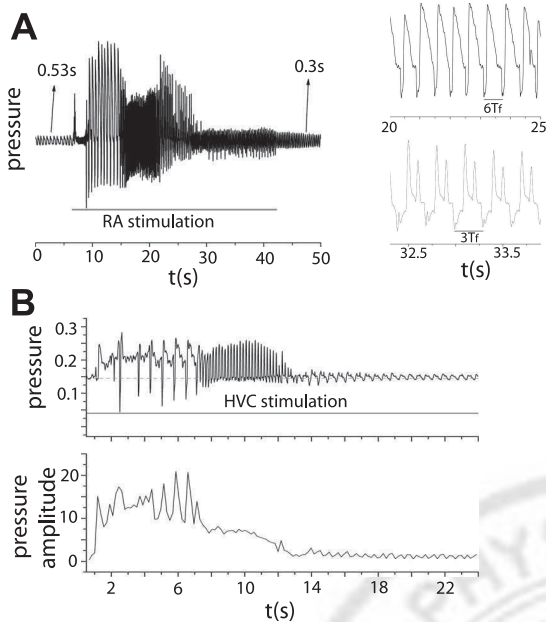


Fig. 3. Transient entrainments obtained in zebra finches. **A**: example of the result of bilateral RA stimulation in a zebra finch (ZF14) with clear transient behavior (period of stimulation is 0.1 s). Different entrainments were obtained as on *right* (time axis indicates the expanded segment), showing a period 6 ($6T_p$) and a period 3 ($3T_p$) entrainment. These periodic pressure patterns were established at different times during the stimulation. For example, the periodic pattern that repeats itself after 6 stimulation periods was observed from between $t = 20$ and 25 s, and the same periodic pattern was repeated 9 times. Stimulation changed the respiratory period from 0.53 to 0.3 s. Gray bar indicates the total duration of the stimulation protocol. **B**: example of transient behavior triggered by HVC stimulation in a zebra finch (ZF13). The transient behavior is associated with high pressure amplitudes. Pressure amplitude was calculated as explained in METHODS, briefly, by first subtracting the ambient pressure from the pressure pattern and then rectifying it. Then basal amplitude for the pressure level was estimated, calculating the average value of the rectified pressure before the stimulation. The “pressure amplitude” was calculated as the average value of the rectified pressure during each stimulation period (0.18 s in this example) divided by the basal level. High values of pressure amplitude (typically because of long and big expiratory pulses) predicted transient behavior.

ment ratios occur rapidly indicates that the neural architecture is also tuned to accomplish fast entrainments (Granada and Herzel 2009).

Lateralized signals are integrated at brain stem respiratory circuitry level. Further strong evidence for interactive control of respiratory rhythms emerged from stimulation protocols using unilateral, synchronous bilateral and alternating bilateral stimulation of the left and right telencephalic vocal control centers. The respiratory network can be entrained by stimulation of either side alone (Fig. 5C). Synchronous bilateral stimulation achieved the same entrainment as unilateral stimulation. Interestingly, alternating stimulation on both sides caused entrainment of the respiratory rhythm to the period of the combined input from both sides (Fig. 5, C and D). This observation demonstrates clearly that the respiratory network integrates input from the left and right telencephalic centers. This nonlateralized interaction is compatible with a model in which the information coming from different hemispheres is integrated and may be redundant for respiratory control.

Minibreaths are reflexively produced. The role of the internal dynamics of the respiratory network was further illustrated with continuous electrical stimulation (Fig. 6). After a period

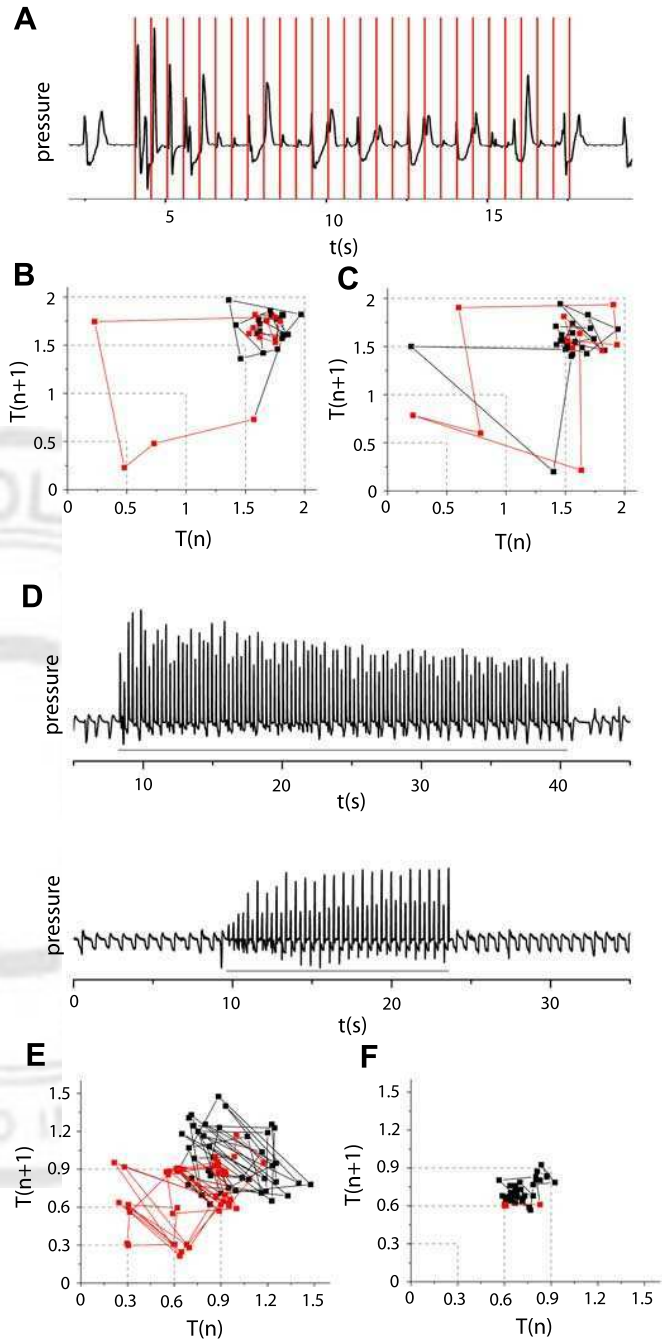
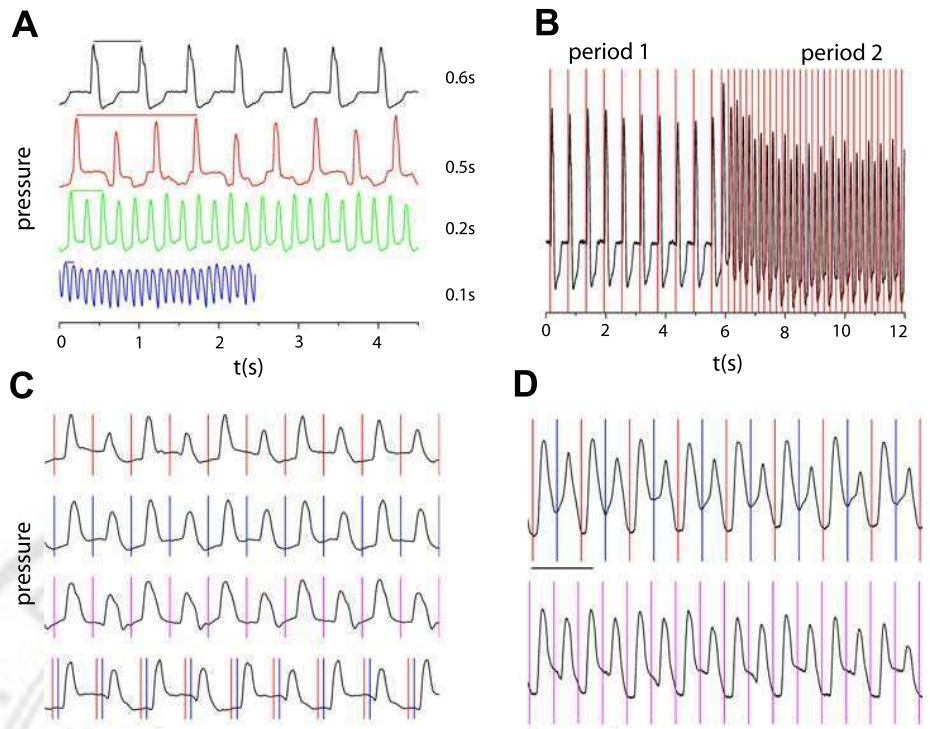


Fig. 4. Entrainments are state dependent. **A**: pressure pattern (black) of a zebra finch (ZF10) under anesthesia showed no entrainment to HVC stimulation (red vertical lines) even at high stimulation currents ($500 \mu A$). **B** and **C**: respiration return maps {the period of a respiratory cycle [$T(n)$] is plotted against its following [$T(n+1)$]} are displayed for $100\text{-}\mu A$ stimulation current (**B**) and for $500 \mu A$ (**C**). Breathing cycles before and after the stimulation are indicated in black, whereas breathing cycles during the stimulation are shown in red. Gray dashed lines indicate the possible entrainments. **D**: pressure patterns for ZF8 while anesthetized (*top*) and awake (*bottom*) showed that $50 \mu A$ was able to entrain respiration in a 1:2 ratio with the stimulation when the bird was awake, but $100 \mu A$ did not result in stable locked responses under anesthesia. In the return maps, the anesthetized bird (**E**) showed high variable breathing periods (black dots and lines) and the lack of stable entrainments (red dots and lines). In the awake bird (**F**), the entrainment is shown by the concentration of all values in one point in the return map because the period was nearly the same for all the cycles.

COGRO

Fig. 5. Entrainment transitions and bilateral control. **A:** telencephalic stimulation entrained respiration. A sequence of entrainments for a canary (CAN4) to different periods of stimulation is shown. The period of the pressure pattern is displayed as a color-coded line above the air sac pressure trace with the corresponding period of the stimulation indicated on *right*. In each case, entrainment followed a change in stimulation frequency and did not require tuning of the stimulation frequency. **B:** rapid change in entrainment of respiratory rhythms followed a change in stimulation frequency in canaries. Changing the period of the stimulation from 0.6 s to 0.2 s produced a change of the entrainment from a period 1 to a period 2 solution. This rapid transition closely resembles those occurring in canary song (Hartley and Suthers 1989). **C** and **D** show the integration of bilateral stimulation by the respiratory circuitry. The pressure patterns obtained with a unilateral (left side in red, right in blue), simultaneous bilateral (purple), or contiguous, sequential bilateral stimulation are similar, implying that the period resulting from integration of both sides determines the respiratory rhythm. Respiratory patterns correspond to a 1:2 entrainment with the stimulation for all stimulation paradigms. In **D**, each side is stimulated in either an alternating or a simultaneous pattern. Keeping the current of the stimulation unchanged, a minimal change of the stimulation period created similar stable entrainments. Scale bars in **C** and **D** indicate 0.5 s.



of continuous activation, which resulted in prolonged high-pressure expirations, short and deep inspirations appeared. These inspirations resemble the inspirations during song (minibreaths; Hartley and Suthers 1989) and are different from deep inspirations during quiet breathing. In some cases these inspirations occurred after the stimulation, which suggests that minibreath-like inspirations emerge as a rebound property of the neural circuitry following a sustained expiration with high pressure amplitude. This emergence of minibreath-like inspirations following long expirations was not the direct result of the driving signal and is therefore suggestive of a feedback-driven intrinsic property of the respiratory circuitry. Consistent with this interpretation, zebra finches independently regulate the duration of song syllables, corresponding to expiratory pressure pulses, and the duration of silent periods, corresponding to minibreaths (Cooper and Goller 2006; Glaze and Troyer 2006). Another interesting observation regarding the pressure pulses obtained as a result of long stimulation trains is that a clear modulation frequency appeared consistent with the activation of RA interneurons, probably creating a synchronized response (Spiro et al. 1999). This high-frequency modulation of the pressure pattern only occurred in zebra finches, and its frequency was lower during anesthesia (Table 2).

During some of the long stimulations (HVC or RA) birds vocalized, but neither vocalizations nor pressure patterns were similar to those during song. In general, the effect of the stimulation was to create a sequence of expiratory pressure pulses and minibreath-like inspirations between them. The first of the stimulated expiratory pulses was of long duration (usually longer than 1 s), much longer than the expiratory pulses of song. Even the following expiratory pulses were longer than those of the song motif. Long-duration stimulation elicited similar respiratory patterns in different individuals and did not reflect differences in the respiratory patterns of their songs.

DISCUSSION

The respiratory patterns following stimulation in the cortical song motor control areas provide unambiguous evidence for interactive processing of the input. The five main lines of evidence are 1) entrainment in subharmonic patterns of the stimulation rhythm; 2) high and low amplitude of pressure pulses, spanning the range from quiet respiration to songlike amplitudes; 3) integration of bilateral input into a single activation regime; 4) emergence of songlike inspirations (minibreaths) after long-duration expiratory pulses of high amplitude are evoked by continuous cortical stimulation; and 5) differences in the effects of the same stimulation regimes on respiratory patterns between awake and anesthetized animals indicate a strong role of inhibitory processes in integration.

In the following we discuss how this experimental paradigm may inform our understanding of telencephalic control of respiration in general. Specific questions to be addressed are the possible locations of this interactive processing, the possible implications of these results for respiratory control during song, and the possible role of feedback mechanisms in this processing.

Where does the observed interactive processing take place? The interactive processing could occur in the respiratory network, in the song control nuclei themselves, or in both locations. The most likely location is the respiratory network. This interpretation derives strong support from the relationship between stimulation frequencies and entrainment patterns relative to the prestimulation respiratory frequency. The fact that it is this relationship between stimulation frequency and respiratory rate at the time of stimulation (Fig. 2) that determines the resulting entrainment is precisely the response that one would expect if a nonlinear respiratory network processes telencephalic input driven by stimulation.

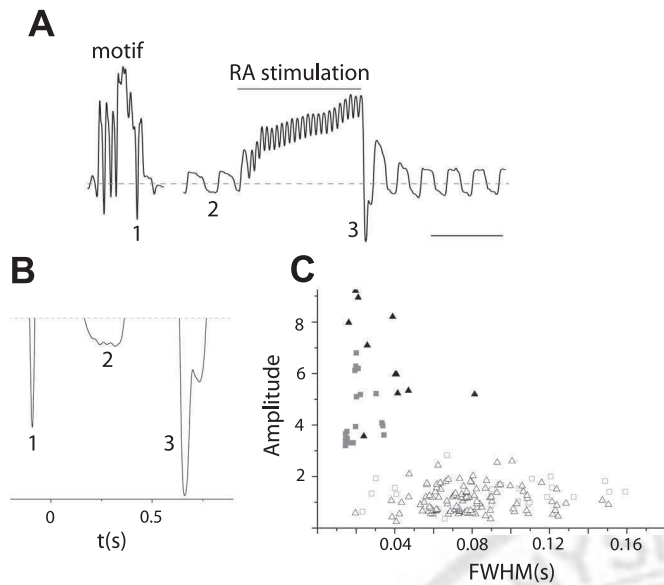


Fig. 6. Effects of continuous long-duration stimulation on pressure patterns. **A:** example of a continuous stimulation in RA for a zebra finch (ZF8). The pressure pattern of its motif is displayed to compare the amplitudes and durations (scale bar, 1 s). The atmospheric level is displayed with a dashed gray line. A minibreath is a deep and very short inspiration during song (1), whereas the pressure pattern of a typical inspiration during quiet breathing is characterized by longer duration and lower amplitude (2). After long continuous stimulation, deep and short inspiration that resembled minibreaths occurred (3). Note the fast frequency component of the response. This is an example of a frequency generated by the circuitry, because its value has no relationship with the stimulation frequency. **B:** detailed air sac pressure pattern of the 3 inspirations labeled in **A**. **C:** amplitude of each inspiration was calculated from atmospheric level and duration as full width at half of this maximal value (FWHM). Squares correspond to naturally occurring respiratory patterns (open, quiet breathing; filled, song); triangles correspond to inspirations following stimulation (open, quiet breathing before and after stimulations; filled, minibreath-like inspirations during and immediately after stimulation).

Processing of the stimulation input could also occur in the telencephalic nuclei themselves. Both HVC and RA contain interneuron networks (Mooney and Prather 2005; Spiro et al. 1999) that could theoretically effect such a response upon stimulation. However, two aspects of our findings are not consistent with an interpretation that the observed entrainment patterns arise from telencephalic processing alone. First, both HVC and RA stimulation resulted in similar respiratory patterns. For this similarity to occur as a result of forebrain processing, it would have to take place in RA and be the same irrespective of whether stimulation occurred in HVC or RA. Alternatively, stimulation in RA would have to cause activation of HVC that is similar to that achieved by its direct stimulation. Furthermore, stimulation in RA at different locations resulted in similar entrainment, making it unlikely that processing within RA alone can account for the observed integration of stimulation into nonlinear respiratory output.

Second, the results from unilateral and bilateral stimulation also make it unlikely that processing in RA and/or HVC alone can explain the observed respiratory response. Considering the suggested pathway for cross-connection (pontine or medullary) between the two motor pathways (Ashmore et al. 2008; Schmidt and Ashmore 2008), a significant delay in activation of >25 ms can be expected, which must interfere with the rhythm of stimulation and thus should generate less consistent

respiratory responses in a stimulation frequency-dependent manner. Furthermore, the interneuron networks of and the ensuing processing in HVC and RA make it unlikely that a unilateral stimulus in either RA or HVC would generate a simple response in the contralateral telencephalic nuclei with identical effects on the respiratory network. It is more plausible to assume that integration at the respiratory network level accounts for the observed respiratory responses.

Although we do not rule out that processing in telencephalic nuclei occurs upon stimulation, the observed patterns of interaction are most parsimoniously explained by integration at the respiratory network level. These observations strongly suggest, therefore, that in this stimulation paradigm the cortical input does not dictate all temporal control but interacts with the intrinsic properties of the respiratory network. Whether the telencephalic signal interacts with the respiratory CPG directly (simple model) or more indirectly (more complex model) cannot be inferred from these data. However, in mammals we have evidence that other brain areas are also involved. Results from studies on sensory stimulations (Potts et al. 2005) and on vocal respiratory coordination (Smotherman et al. 2006) suggest that the parabrachial nucleus is a fundamental part of the circuitry in mammals.

Implications for respiratory control during song production. The results presented here raise the question of whether an integrative mechanism, similar to that during the experimental stimulation, may be employed during spontaneous song production or whether a principally different control mechanism occurs as has been suggested (Fee et al. 2004). Several key features of respiration during song emerged also as a result of cortical stimulation. First, the elevated amplitude of expiratory and inspiratory pressure pulses and short duration of deep inspirations (minibreaths) match those observed during song. Second, species differences in the respiratory response to stimulation are consistent with differences in the temporal organization of song and the corresponding respiratory patterns in zebra finches (no repeated syllables) and canaries (repetition of syllables into phrases is the rule). This difference suggests that the requirements for temporal structure in the control signals from the forebrain to the respiratory centers may also

Table 2. Fast frequency caused by continuous stimulation

Bird	Stimulation Site	State	Frequency, Hz
ZF7	RA: bilateral	Anesthetized	No fast frequency
ZF8	RA: right	Anesthetized	4.2 ± 0.2
ZF10	HVC: left	Anesthetized	No fast frequency
ZF11	HVC: left	Anesthetized	No fast frequency
ZF15	RA left	Anesthetized	7.4 ± 0.3
ZF4	RA: left	Chronic	14.1 ± 1.3
ZF5	RA: right	Chronic	13.5 ± 0.7
ZF6	RA: right	Chronic	12.5 ± 0.9
ZF8	RA: right	Chronic	12.6 ± 0.6
ZF9	HVC: left	Chronic	13.5 ± 1
ZF13	HVC: right	Chronic	9.4 ± 0.4
ZF14	RA: right	Chronic	15.4 ± 0.7
ZF14	RA: left	Chronic	14.2 ± 0.6
ZF14	RA bilateral	Chronic	15.7 ± 0.5
CAN1	RA: right	Anesthetized	No fast frequency
CAN2	RA: right	Chronic	No fast frequency
CAN3	RA: left	Chronic	No fast frequency
CAN4	HVC bilateral	Chronic	No fast frequency
CAN5	HVC: left	Chronic	No fast frequency

be different, possibly paralleling differences in the generation of discrete and rhythmic movements in mammals (Ikegami et al. 2010; Schaal et al. 2004). Lack of stable, sustained rhythms in the song of the zebra finch may require more directive input than the driving of intrinsic rhythms emerging from the non-linear network in the canary. Third, the emergence of a respiratory response to varying stimulation rhythms in the Arnold tongue pattern is consistent with respiratory patterns during song in the canary (Trevisan et al. 2006a). Fourth, respiratory integration of bilateral input is consistent with an absence of lateralized control of respiration during song (Goller and Suthers 1999). In view of these parallels, it is most parsimonious to assume that the interactive mechanism is also employed during song. However, because respiration during song also includes features that were not observed during stimulation protocols, it is clear that motor control of spontaneously produced song requires more detailed telencephalic input and more complex integrative processing than that induced by the simple stimulation regimes used in this study.

This conclusion does not support a view that HVC output directly controls all temporal aspects of song, i.e., expiratory modulation and timing of expirations and inspirations. This direct-control model was based on documentation of firing patterns of HVC neurons (Hahnloser et al. 2002) and the results of HVC cooling on song tempo (Andalman et al. 2011; Long and Fee 2008). However, our approach does not directly address these experiments but challenges their interpretation by providing supporting evidence for an alternative, interactive model (Trevisan et al. 2006a). Importantly, the interactive model is not inconsistent with the sparse firing of HVC neurons that project to RA or the results of the cooling experiment. Sparse activity could interact with the respiratory circuitry without having to encode every temporal aspect of song. In the same way, the internal dynamics of a system could filter certain features of an input signal (for example in the frequency space). Nonlinear systems can create complexity with very simple input signals (Eguia et al. 2000). The results of this experiment therefore do not take issue with the sparse firing in HVC neurons but merely provide a plausible, different understanding of its role. Even though the possibility of recreating songlike expiratory and inspiratory pulses by a broad stimulation speaks against a requirement for very specific input signals, it is possible that the main features of the motor gestures for song are coded at a population level (implied by the integration displayed by the respiratory system), with some of the details emerging from firing patterns of specific neurons. Moreover, here we address only respiratory control, and the generation of the syringeal instructions may involve additional control mechanisms. A nonlinear integration between the activity of respiratory nuclei and telencephalic instructions is not incompatible with the stretching of the outcome as the telencephalic timing is slowed down (as described in Long and Fee 2008; Andalman et al. 2011). Notably, the signature of integration used here is the existence of subharmonic locking, which occurs in a wide region of the forcing parameter space (forcing frequency and amplitude).

Comparison with other cortical control mechanisms of downstream motor circuits. How cortical control interacts with motor circuits in directing behavior is a general question in motor control. Although the control mechanisms will be specific for each system, this research illustrates a potential,

general mechanism for generating diversity and complexity through interaction of different systems. Clear parallels exist between respiratory control documented here and the cortical control of other motor behaviors. For example, the control of whisking in rats may involve interactions between oscillatory rhythms in a cerebellar nucleus (inferior olivary nucleus) and modulatory instructions from the motor cortex (Lang et al. 2006; Marshall and Lang 2004). Interestingly, whisker movements display subharmonic entrainments when the motor cortex is stimulated, consistent with the oscillatory behavior of the cerebellar area (Lang et al. 2006). An alternative proposal envisions the role of the motor cortex as modulating a subcortical CPG (Cramer and Keller 2006). A similar model for the generation of the motor gestures for song has been proposed, in which the respiratory system with its dynamics gives rise to part of the complex temporal features (Alliende et al. 2010; Mendez et al. 2006; Trevisan et al. 2006a). For canaries, respiratory gestures during song and quiet breathing were recreated with this model, using simple telencephalic instructions, and much of the complexity of the gestures therefore arises from the interaction and need not be present in telencephalic signals (Trevisan et al. 2006a, 2006b). It is also likely that similar interactive processing is used in learned vocal behavior of mammals and therefore in humans. In the case of respiration, the interaction between voluntary modification of an involuntary physiological control network may be constrained by the life-sustaining functions and thus favor the evolution of integrated control. Although cortical control of other motor behaviors may not be subjected to similarly strong constraints, integrative processing may still be the most common mechanism for control of rhythm-generating networks.

Experiments in a mammalian vocal system, in which regions of motor cortex involved in the volitional control of respiration exist, applied different stimulation methods and protocols, making a direct comparison difficult. Nevertheless, during transcranial magnetic stimulation of the cortical areas involved in volitional control of respiration in humans, no cortico-bulbar pathway seemed to be activated, so that the stimulation resulted in an activation of the diaphragm with no effect on the respiratory phase (Corfield et al. 1998). In our experiment, the single train of stimulation in RA (Fig. 1C) clearly changed the respiratory dynamics, indicating an interaction of the telencephalic signal with the internal dynamics of the respiratory system. In other mammalian models a similar experimental approach was used to study cortical control of movements. Short pulse trains of electrical stimulation in the motor and premotor cortex in monkeys induced muscle twitches (e.g., Asanuma et al. 1976; Strick and Preston 1978) and behaviorally relevant complex movements when the duration of the pulse train was comparable to the actual natural behavior (Graziano et al. 2002).

In our experiments short pulse trains also directly affected expiratory muscles (similar to Graziano et al. 2002), but the long stimulation train did not produce songlike pressure patterns. This is in contrast to a previous study (Vicario and Simpson 1995), in which continuous stimulation trains triggered vocalizations with some similarities to the learned vocalizations. However, while the activated behavior in monkeys started immediately after the beginning of the stimulation (Graziano et al. 2002), in birds the behavior emerged only after long latencies (Vicario and Simpson 1995). Here we show that

AQ: 5

long stimulation trains rapidly caused pressure pulses with increased amplitude that did not trigger vocalizations. Because only sound was recorded in the earlier study (Vicario and Simpson 1995), this influence on respiration could not be detected. Long latencies to actual sound production may arise from a facilitation of different neural networks and from more indirect activation of the vocal motor systems. It is unclear whether the differences in these two examples of cortical control of motor functions in birds and mammals arise from a difference in motor task (arm movement vs. respiration) or a different mechanism of interaction between cortical areas and motor areas. However, whereas cortico-spinal connections are well documented in mammals for several motor systems, including respiration (e.g., Butler 2007; Corfield et al. 1998; Haouzi and Bell 2009; Lemon 2008), in songbirds no direct connection from HVC or RA to the motor neurons of respiratory muscles is known.

Implications for the use of feedback. The interaction between telencephalic areas and the respiratory system (Fig. 2) and the existence of a clear phase relationship for the effect of the stimulation on respiration (Fig. 1) provide strong support for a model that proposes the use of information flow from the respiratory network to the telencephalic song control areas (Ashmore et al. 2008; Schmidt and Ashmore 2008). Respiratory information from the brain stem is routed to HVC, and feedback from the periphery is actively used during song (Ashmore et al. 2008; Suthers et al. 2002). The existence of feedback loops increases the stability of the motor program and coordinates the telencephalic-brain stem interaction. Ashmore et al. (2008) documented a bilateral thalamic connection from the respiratory areas of the brain stem to HVC. Here we show that bilateral signals are integrated in the respiratory circuitry and that respiratory dynamics are not very sensitive to hemispheric origin of the input. This evidence, together with bilateral feedback routes, supports the idea that the respiratory control network acts as a general integrator of bilateral timing input. This mechanism of operation in a nonlinear fashion is contrasted with a more linear processing in other motor systems. For example, circuitry in the cat motor cortex (Ethier et al. 2006) uses nearly linear addition of spatially separated stimulation for control of paw movement. We found that respiratory dynamics do not reflect a simple linear addition of input from both hemispheres. Sensory feedback could directly or indirectly influence the coordination of rhythms by influencing the respiratory network or by influencing the relay nuclei in brain stem areas. These effects can incorporate different timescales from fast (when the respiratory dynamics is directly affected) to a more modulatory role (with more indirect effects). A model in which all the timing details of the song are internally fixed in HVC would not make use of any of these feedback options.

An interesting effect observed in this work was the lack of coordination between the telencephalic rhythm and respiration under anesthesia. In the latter condition, the entrainments could only be maintained for a short time. In general, the effect of anesthesia is suppressive. For example, it was shown that anesthesia decreases the size of the evoked whisker movement (Berg and Kleinfeld 2003; Brecht et al. 2004). In line with these experiments, anesthesia in our study produces an inhibition of motor output and a clear desynchronization of stimulation and respiratory activity. The difference in the degree of

coordination might be caused by reduced cortical input on brain stem areas, by variability observed in the breathing pattern during anesthesia, or by a combination of both mechanisms. The transition from anesthesia to the awake state, represented by a disinhibition of the motor output, resulted in an increased degree of coordination. Disinhibition therefore potentiates coordination, which makes its use during song highly plausible.

Low-dimensional systems may be used widely in central neural control. A common strategy in nonlinear dynamics for understanding the behavior of a system is to explore its dynamics under a periodical forcing of one variable. For example, periodical forcing of a CPG in the pyloric stomatogastric ganglion of the lobster (Szücs et al. 2001), showed that this complex, but still small, set of interconnected neurons displays a dynamical repertoire compatible with a low-dimensional system (i.e., the dynamics of the system is described by a small set of variables) and that the rhythms emerge as cooperative outputs. Respiratory control in vertebrates involves a much more complex neural network, but our experiment and theoretical work suggest that complex networks could still display features of low-dimensional dynamics (Alonso et al. 2009; Ott and Antonsen 2008). More complete models for respiratory control are starting to emerge in mammals (Rubin et al. 2009; Rybak et al. 2004; Smith et al. 2009), and subharmonic behavior is an essential component of integrating respiration with other rhythmic behaviors, such as locomotion (e.g., Bramble and Carrier 1983; Funk et al. 1992; Potts et al. 2005). Assuming parallels in respiratory control between birds and mammals, the use of low-dimensional dynamics may be a general mechanism of integration. How a big population of neurons displays low-dimensional dynamics (Alonso et al. 2009; Ott and Antonsen 2008) is a key question for future research. It is clear, however, that these interactive properties of diverse sets of neurons with their intrinsic nonlinearities (Kubke et al. 2005) must be considered in our pursuit of understanding of respiratory control of vocal behavior.

GRANTS

This work was supported by National Institute on Deafness and Other Communications Disorders Grant DC-06876. **AQ: 6**

DISCLOSURES

No conflicts of interest, financial or otherwise, are declared by the author(s). **AQ: 7**

AUTHOR CONTRIBUTIONS

Author contributions: J.M.M., G.B.M., and F.G. conception and design of research; J.M.M. performed experiments; J.M.M. analyzed data; J.M.M., G.B.M., and F.G. interpreted results of experiments; J.M.M. prepared figures; J.M.M., G.B.M., and F.G. drafted manuscript; J.M.M., G.B.M., and F.G. edited and revised manuscript; J.M.M., G.B.M., and F.G. approved final version of manuscript.

REFERENCES

- Ahrens KF, Kleinfeld D. Current flow in vibrissa motor cortex can phase-lock with exploratory rhythmic whisking in rat. *J Neurophysiol* 92: 1700–1707, 2004.
- Alliende JA, Méndez JM, Goller F, Mindlin GB. Hormonal acceleration of song development illuminates motor control mechanism in canaries. *Dev Neurobiol* 70: 943–960, 2010.

- Alonso LM, Allende JA, Goller F, Mindlin GB.** Low-dimensional dynamical model for the diversity of pressure patterns used in canary song. *Phys Rev E* 79: 041929, 2009.
- Andalman AS, Foerster JN, Fee MS.** Control of vocal and respiratory patterns in birdsong: dissection of forebrain and brainstem mechanisms using temperature. *PLoS One* 6: e25461, 2011.
- Asanuma H, Arnold A, Zarzecki P.** Further study on the excitation of pyramidal tract cells by intracortical microstimulation. *Exp Brain Res* 26: 443–461, 1976.
- Ashmore RC, Wild JM, Schmidt MF.** Brainstem and forebrain contributions to the generation of learned motor behavior for song. *J Neurosci* 25: 8543–8534, 2005.
- Ashmore RC, Renk JA, Schmidt MF.** Bottom up activation of the vocal motor forebrain by the respiratory brainstem. *J Neurosci* 28: 2613–2623, 2008.
- Berg RW, Kleinfeld D.** Vibrissa movement elicited by rhythmic electrical microstimulation to motor cortex in the aroused rat mimics exploratory whisking. *J Neurophysiol* 90: 2950–2963, 2003.
- Bramble DN, Carrier DR.** Running and breathing in mammals. *Science* 219: 251–256, 1983.
- Brecht M, Schneider M, Sakmann B, Margrie TW.** Whisker movements evoked by stimulation of single pyramidal cells in rat motor cortex. *Nature* 427: 704–710, 2004.
- Butler JE.** Drive to the human respiratory muscles. *Respir Physiol Neurobiol* 159: 115–126, 2007.
- Capaday C.** The integrated nature of motor cortical function. *Neuroscientist* 10: 207–220, 2004.
- Cooper BG, Goller F.** Physiological insights into social-context-dependent changes in the rhythm of the song motor program. *J Neurophysiol* 95: 3798–3809, 2006.
- Corfield DR, Murphy K, Guz A.** Does the motor control of the diaphragm “bypass” the brain stem respiratory centres in man? *Respir Physiol* 114: 109–117, 1998.
- Cramer NP, Keller A.** Cortical control of whisking central pattern generator. *J Neurophysiol* 96: 209–217, 2006.
- Eguia MC, Rabinovich MI, Abarbanel HD.** Information transmission and recovery in neural communications channels. *Phys Rev E* 62: 7111–7122, 2000.
- Ethier C, Brizzi L, Darling WG, Capaday C.** Linear summation of cat motor cortex outputs. *J Neurosci* 26: 5574–5581, 2006.
- Fee MS, Kozhevnikov AA, Hahnloser RH.** Neural mechanisms of vocal sequence generation in the songbird. *Ann NY Acad Sci* 1016: 153–170, 2004.
- Feingold M, Gonzalez DL, Piro O, Viturro H.** Phase locking, period doubling, and chaotic phenomena in externally driven excitable systems. *Phys Rev A* 37: R4060, 1988.
- Friedman WA, Jones LM, Cramer NP, Kwegyir-Afful EE, Zeigler HP, Keller A.** Anticipatory activity of motor cortex in relation to rhythmic whisking. *J Neurophysiol* 95: 1274–1277, 2006.
- Funk GD, Steeves JD, Milsom WK.** Coordination of wingbeat and respiration in birds. II. “Fictive” flight. *J Appl Physiol* 73: 1025–1033, 1992.
- Glass L.** Synchronization and rhythmic processes in physiology. *Nature* 410: 277–284, 2001.
- Glaze CM, Troyer TW.** Temporal structure in zebra finch song: implications for motor coding. *J Neurosci* 26: 991–1005, 2006.
- Goller F, Cooper BG.** Peripheral motor dynamics of song production in the zebra finch. *Ann NY Acad Sci* 1016: 130–152, 2004.
- Goller F, Suthers RA.** Role of syringeal muscles in gating airflow and sound production in singing brown thrashers. *J Neurophysiol* 75: 867–876, 1996a.
- Goller F, Suthers RA.** Role of syringeal muscles in controlling the phonology of bird song. *J Neurophysiol* 76: 287–300, 1996b.
- Goller F, Suthers RA.** Bilaterally symmetrical respiratory activity during lateralized birdsong. *J Neurobiol* 41: 513–523, 1999.
- Gonzalez DL, Piro O.** Chaos in a nonlinear driven oscillator with exact solution. *Phys Rev Lett* 50: 870, 1983.
- Granada AE, Herzog H.** How to achieve fast entrainment? The timescale of synchronization. *PLoS One* 4: e7057, 2009.
- Graziano MS, Taylor CS, Moore T.** Complex movements evoked by microstimulation of precentral cortex. *Neuron* 34: 841–851, 2002.
- Hahnloser RH, Kozhevnikov AA, Fee MS.** An ultra-sparse code underlies the generation of neural sequences in a songbird. *Nature* 419: 65–70, 2002.
- Haouzi P, Bell HJ.** Control of breathing and volitional respiratory rhythm in humans. *J Appl Physiol* 106: 904–910, 2009.
- Hartley RS, Suthers RA.** Airflow and pressure during canary song: evidence for mini-breaths. *J Comp Physiol A* 165: 15–26, 1989.
- Histed MH, Bonin V, Reid RC.** Direct activation of sparse, distributed populations of cortical neurons by electrical microstimulation. *Neuron* 63: 508–522, 2009.
- Ikegami T, Hirashima M, Taga G, Nozaki D.** Asymmetric transfer of visuomotor learning between discrete and rhythmic movements. *J Neurosci* 30: 4515–4521, 2010.
- Kakei S, Hoffman DS, Strick PL.** Muscle and movement representations in the primary motor cortex. *Science* 285: 2136–2139, 1999.
- Kubke MF, Yazaki-Sugiyama Y, Mooney R, Wild JM.** Physiology of neuronal subtypes in the respiratory-vocal integration nucleus retroambiguus of the male zebra finch. *J Neurophysiol* 94: 2379–2390, 2005.
- Lang EJ, Sugihara I, Llinás R.** Olivocerebellar modulation of motor cortex ability to generate vibrissal movements in rat. *J Physiol* 571.1: 101–120, 2006.
- Lemon LN.** Descending pathway in motor control. *Annu Rev Neurosci* 31: 195–218, 2008.
- Long MA, Fee MS.** Using temperature to analyze temporal dynamics in the songbird motor pathway. *Nature* 456: 189–194, 2008.
- Marshall SP, Lang EJ.** Inferior olive oscillations gate transmission of motor cortical activity to the cerebellum. *J Neurosci* 24: 11356–11367, 2004.
- Mendez JM, Allende JA, Amador A, Mindlin GB.** Dynamical systems techniques reveal the sexual dimorphic nature of motor patterns in birdsong. *Phys Rev E* 74: 041917, 2006.
- Miller AD, Bianchi AL, Bishop BP.** *Neural Control of the Respiratory Muscles*. Boca Raton, FL: CRC, 1997.
- Mooney R, Prather JF.** The HVC microcircuit: the synaptic basis for interactions between song motor and vocal plasticity pathways. *J Neurosci* 25: 1952–1964, 2005.
- Osipov GV, Kurths J, Zhou C.** *Synchronization in Oscillatory Networks*. Berlin: Springer, 2007.
- Ott E, Antonsen TM.** Low dimensional behavior of large systems of globally coupled oscillators. *Chaos* 18: 037113, 2008.
- Pipes LA, Harvill LR.** *Applied Mathematics for Engineers and Physicists*. Tokyo: McGraw Hill, 1949.
- Potts JT, Rybak IA, Paton JFR.** Respiratory rhythm entrainment by somatic afferent stimulation. *J Neurosci* 25: 1965–1978, 2005.
- Rekling JC, Feldman JL.** PreBötzing complex and pacemaker neurons. *Annu Rev Physiol* 60: 385–405, 1998.
- Riddle CN, Baker SN.** Convergence of pyramidal and medial brain stem descending pathways onto macaque cervical spinal interneurons. *J Neurophysiol* 103: 2821–2832, 2010.
- Rubin JE, Shevtsova NA, Ermentrout GB, Smith JC, Rybak IA.** Multiple rhythmic states in a model of the respiratory central pattern generator. *J Neurophysiol* 101: 2146–2165, 2009.
- Rybak IA, Shevtsova NA, Paton JF, Dick TE, St-John WM, Mörschel M, Deutschmann M.** Modeling the ponto-medullary respiratory network. *Respir Physiol Neurobiol* 143: 307–319, 2004.
- Schaal S, Sternad D, Osu R, Kawato M.** Rhythmic arm movement is not discrete. *Nat Neurosci* 7: 1137–1144, 2004.
- Schmidt MF, Ashmore R.** Integrating breathing and singing: forebrain and brainstem mechanisms. In: *Neuroscience of Birdsongs*, edited by Zeigler HP, Marler P. Cambridge, UK: Cambridge Univ. Press, 2008, p. 115–135.
- Smith JC, Abdala AP, Rybak IA, Paton JF.** Structural and functional architecture of respiratory networks in the mammalian brainstem. *Philos Trans R Soc Lond B Biol Sci* 364: 2577–2587, 2009.
- Smotherman M, Kobayasi K, Ma J, Zhang S, Metzner W.** A mechanism for vocal-respiratory coupling in the mammalian parabrachial nucleus. *J Neurosci* 26: 4860–4869, 2006.
- Soto O, Cros D.** Direct corticospinal control of force derivative. *J Neurosci* 31: 1944–1948, 2011.
- Spiro JE, Dalva MB, Mooney R.** Long-range inhibition within the zebra finch song nucleus RA can coordinate the firing of multiple projection neurons. *J Neurophysiol* 81: 3007–3020, 1999.
- Strick PL, Preston PB.** Multiple representation in the primate motor cortex. *Brain Res* 154: 366–370, 1978.
- Suthers RA, Goller F, Pytte C.** The neuromuscular control of birdsong. *Philos Trans R Soc Lond B Biol Sci* 354: 927–939, 1999.
- Suthers RA, Goller F, Wild JM.** Somatosensory feedback modulates the respiratory motor program of crystallized birdsong. *Proc Natl Acad Sci USA* 99: 5680–5685, 2002.
- Suthers RA, Vallet E, Tanvez A, Kreutzer M.** Bilateral song production in domestic canaries. *J Neurobiol* 60: 381–393, 2004.

- Szücs A, Elson RC, Rabinovich MI, Abarbanel HD, Selverston AI.** Nonlinear behavior of sinusoidally forced pyloric pacemaker neurons. *J Neurophysiol* 85: 1623–1638, 2001.
- Trevisan MA, Goller F, Mindlin GB.** Nonlinear model predicts diverse respiratory patterns of birdsong. *Phys Rev Lett* 96: 058103, 2006a.
- Trevisan MA, Mendez JM, Mindlin GB.** Respiratory patterns in oscine birds during normal respiration and song production. *Phys Rev E* 73: 061911, 2006b.
- Vicario DS.** Organization of the zebra finch song control system. II. Functional organization of outputs from nucleus robustus archistriatalis. *J Comp Neurol* 309: 486–494, 1991.
- Vicario DS, Simpson HB.** Electrical stimulation in forebrain nuclei elicits learned vocal patterns in songbirds. *J Neurophysiol* 73: 2602–2607, 1995.
- Wiggins S.** *Introduction to Applied Nonlinear Dynamical Systems and Chaos*. New York: Springer, 2003.
- Wild JM.** Neural pathways for the control of birdsong production. *J Neurobiol* 33: 653–670, 1997.
- Wild JM, Kubke MF, Mooney R.** Avian nucleus retroambigualis: cell types and projections to other respiratory-vocal nuclei in the brain of the zebra finch (*Taeniopygia guttata*). *J Comp Neurol* 512: 768–783, 2009.
- Zeigler HP, Marler P.** *Neuroscience of Birdsong*. Cambridge, UK: Cambridge Univ. Press, 2008.

